

# Systematic Variations in Stress State in the Southern San Joaquin Valley: Inferences Based on Well-Bore Data and Contemporary Seismicity: Special Supplement

David A. Castillo and Mark D. Zoback<sup>1</sup>

Figure 1a is a schematic illustrating the stress drop associated with reverse slip during an earthquake. Note that the sense of stress drop is opposite to that of the slip event. The stress drop,  $\tau_D$ , averaged over the ruptured fault surface, can be described in terms of a stress tensor,  $S$  in the coordinate system shown in Figure 1a.

$$S = \begin{bmatrix} 0 & 0 & \tau_D \\ 0 & 0 & 0 \\ \tau_D & 0 & 0 \end{bmatrix} \quad (1)$$

The induced pure shear stress can be equivalently expressed in terms of principal stress magnitudes and directions using the following expression after Jaeger and Cook (1979),

$$\begin{aligned} \sigma_1 &= -\tau_D \\ \sigma_3 &= +\tau_D \end{aligned} \quad (2)$$

where  $\sigma_1$  and  $\sigma_3$  are the induced principal stress magnitudes (positive compression). Note that the principal stress directions for this equivalent stress tensor would be oriented  $45^\circ$  with respect to the fault plane. The equivalent stress tensor,  $S'$  producing pure shear in the  $x'y'z'$  coordinate system (Figure 1b), is

$$S' = \begin{bmatrix} -\tau_D & 0 & 0 \\ 0 & 0 & 0 \\ 0 & 0 & \tau_D \end{bmatrix} \quad (3)$$

To investigate whether the earthquake-induced stress drop could alter the remote stress field, we transform the induced stress tensor into the horizontal and vertical reference frame (i.e.,  $x''y''z''$  in Figure 1b) by correcting for the fault dip,  $\theta$ . This transformation (Malvern, 1969) representing a rotation of angle  $\beta$  about the  $y'$  axis is shown below,

$$B = \begin{bmatrix} \cos\beta & 0 & -\sin\beta \\ 0 & 1 & 1 \\ \sin\beta & 0 & \cos\beta \end{bmatrix} \quad (4)$$

where  $\beta = \theta - \pi/4$ .

An additional transformation places the  $x''y''z''$  coordinate system into the remote stress field coordinate system. This rotation amounts to an angle  $\delta$  about the  $z''$  axis, corresponding to the difference between the orientation of the normal to the fault strike and the remote maximum principal stress direction as shown in Figure 1c. This tensor transformation is,

$$D = \begin{bmatrix} \cos\delta & \sin\delta & 0 \\ -\sin\delta & \cos\delta & 0 \\ 0 & 0 & 1 \end{bmatrix} \quad (5)$$

The net transformation of the earthquake-induced stress field into the remote stress field active prior to the 1952 earthquake can be produced by multiplying the matrices in equations 3 to 5 as shown below:

$$S^* = [D] [B] [S'] [B]^T [D]^T \quad (6)$$

The resultant stress field ( $\sigma^*$ ) is simply the sum of the rotated earthquake-induced stress tensor (equation 6) and the remote stress tensor, whose components are  $\sigma_{xx} = S_{Hmax}$ ,  $\sigma_{yy} = S_{hmin}$ ,  $\sigma_{xy} = 0$  as shown below:

$$\begin{aligned} \sigma_{xx}^* &= S_{Hmax} + S_D \left( \sin^2 \beta \cos^2 \delta - \cos^2 \beta \cos^2 \delta \right) \\ \sigma_{yy}^* &= S_{hmin} + S_D \left( \sin^2 \beta \sin^2 \delta - \cos^2 \beta \sin^2 \delta \right) \\ \sigma_{xy}^* &= S_D \sin \delta \cos \delta \left( 2 \cos^2 \beta - 1 \right) \end{aligned} \quad (7)$$

The angle difference ( $\gamma$ ) reflecting the change in the principal stress orientation can be obtained using the following:

$$\tan 2\gamma = \frac{2\sigma_{xy}^*}{\sigma_{xx}^* - \sigma_{yy}^*} \quad (8)$$

Substituting expressions in equation 7 into equation 8 and solving for  $S_{Hmax} - S_{hmin}$ , the difference in the remote horizontal principal stresses yields,

$$S_{Hmax} - S_{hmin} = S_D \left\{ \left( 2 \cos^2 \beta - 1 \right) \left( \frac{\sin 2\delta}{\tan 2\gamma} + 2 \cos^2 \beta - 1 \right) \right\} \quad (9)$$

Assuming the crust is in frictional equilibrium, slip along optimally oriented faults will occur when the ratio of the maximum to minimum effective principal stresses exceeds a value determined by the frictional strength of the crust in the following equation after Jaeger and Cook (1979),

$$\frac{S_1 - P_O}{S_3 - P_O} \leq \left[ (\mu^2 + 1)^{1/2} + \mu \right]^2 \quad (10)$$

where  $\mu$  is the coefficient of friction, and  $P_O$  is pore pressure. That the southern San Joaquin Valley is primarily dominated by reverse faulting and active folding with east-west trending axes (Webb and Kanamori, 1985; Davis and Lague, 1986) implies a stress regime where  $S_1 = S_{Hmax}$ ,  $S_2 = S_{hmin}$ , and  $S_3 = S_V$ . Using equation 10 to estimate  $S_{Hmax}$  ( $S_1$ ), and considering the depth of 4 km (mean depth of the breakout measurements), we estimate  $S_V$  using a rock density of 2300 kg/m<sup>3</sup> and hydrostatic pore pressure. Using a coefficient of friction of  $\mu = 0.6$ , a value falling within the range of observations made by Byerlee (1979) for a wide variety of rock types, we find that  $S_{Hmax} = 196$  MPa. Using equation 9, we estimate the horizontal stress differences given the fault geometry and the stress field in the southern San Joaquin Valley (Figure 12 in Castillo and Zoback, 1994). Assuming a stress drop of  $\tau_D \approx 80$  MPa (Kanamori and Anderson, 1975),  $\beta = 5^\circ$  (corresponding to  $\theta = 50^\circ$ ),  $\delta = 30^\circ$  (roughly the difference between the fault strike of N70°E and the remote  $S_{Hmax}$  stress direction inferred from the Yowlumne and Rio Viejo fields), and  $\gamma = 35^\circ$  ( $S_{Hmax}$  stress perturbation seen in the San Emidio and Pleito fields), we find that  $S_{Hmax} - S_{hmin} = 10$  MPa. The magnitude of  $S_{hmin}$  at a depth of 4 km is therefore about 186 MPa, indicating that the horizontal stresses are comparable in magnitude.

The slip vector for a given earthquake, assuming the direction is the direction of maximum shear stress, is primarily a function of several parameters, which include (1) the orientation of the remote stress field, (2) the orientation of the fault plane, and (3) the relative magnitudes of the principal stresses. Relative stress magnitudes can be described in terms of the relative stress relation,  $\phi$  after Angelier (1979),

$$\phi = \frac{S_2 - S_3}{S_1 - S_3} \quad (11)$$

where  $\phi$  varies from 0 to 1. For a reverse stress regime,  $\phi = 1$  corresponds to  $S_{Hmax} = S_{hmin}$ , a stress regime that supports pure reverse faulting. When  $\phi = 0$ , corresponding to  $S_{hmin} = S_V$ , a combined reverse and strike-slip faulting stress regime occurs. The inferred magnitudes of the principal stresses estimated from the 1952 earthquake stress drop and the measured stress directions indicates that  $\phi \sim 0.9$ .

In general, equation 9 allows us to examine the range of possible horizontal stress differences ( $S_{Hmax} - S_{hmin}$ ) necessary to satisfy a given earthquake (i.e.,  $\beta$  and  $\tau_D$ ) as a function of the stress perturbations,  $\gamma$ . The results are shown in Figure 16 in Castillo and Zoback (1994) using the Wallace and Junkyoung (1989) southwest fault model where  $\beta = 5^\circ$  (fault dip of  $\theta = 50^\circ$ ). Accounting for any possible uncertainties in strike of the ruptured fault, N70°E  $\pm$  10° Wallace and Junkyoung, 1989, and the orientation of the remote stress field (N10°E  $\pm$  10°), we varied the angular difference,  $\delta$ , between the projected earthquake-induced and remote stress directions from  $\delta = 10^\circ$ ,  $30^\circ$ , and  $50^\circ$ . Results for the fault models tested indicate that for  $\gamma > 20^\circ$  the  $S_{Hmax} - S_{hmin}$  stress difference must be less than 30 MPa (Figure 16 in Castillo and Zoback 1994), corresponding to  $\phi \geq 0.75$ . Since  $\gamma$  ranges from  $30^\circ$  to  $50^\circ$ , it appears that the difference between  $S_{Hmax}$  and  $S_{hmin}$  may also range from 10 to 30 MPa (Figure 16 in Castillo and Zoback 1994), corresponding to  $\phi$  ranging from 0.7 to 0.9.

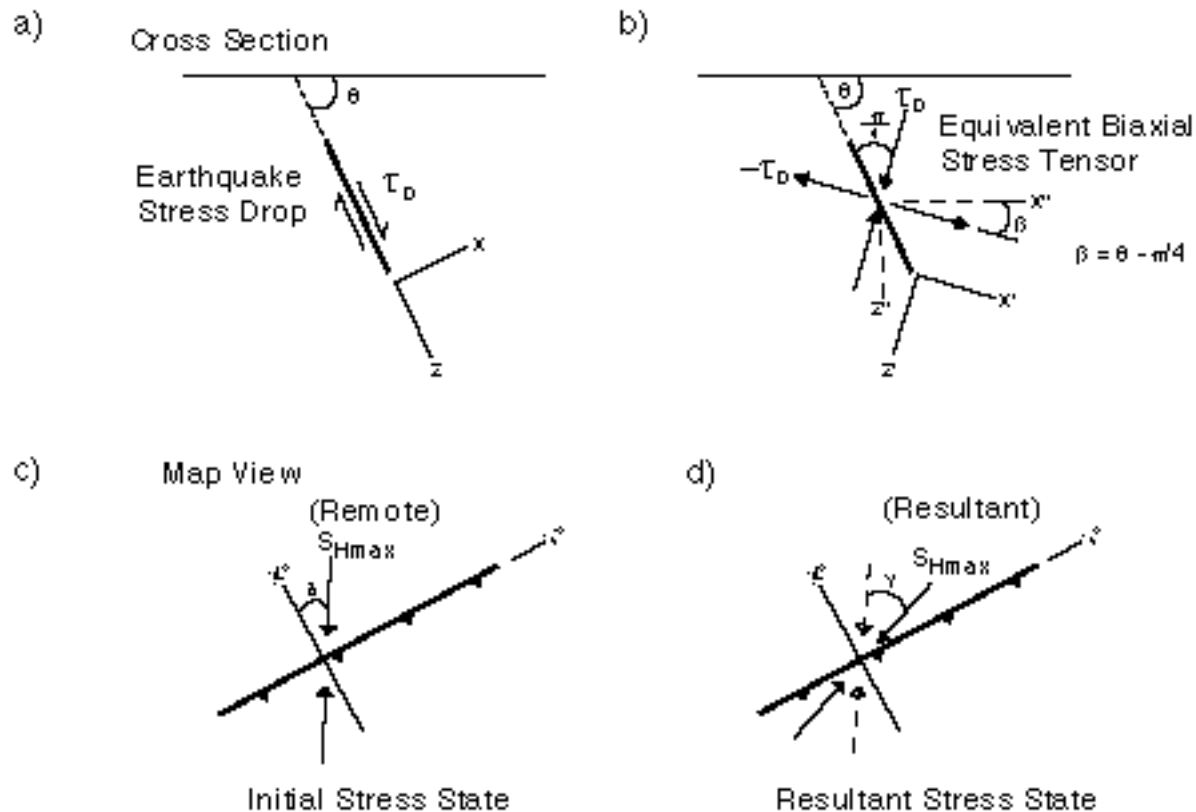


**Figure 1 – Illustration of the geometry and coordinate systems used in the tensor transformation for superimposing the earthquake-induced stress drop ( $\tau_D$ ) with the remote stress field ( $S_{Hmax}$ ).** (a) The cross section illustration starts with the shear stress acting in the opposite sense signifying the earthquake stress drop,  $\tau_D$ . (b) The equivalent biaxial stress tensor to the pure shear stress drop undergoes the necessary rotation ( $\beta$ ) needed to put the principal stresses in the horizontal and vertical planes. Note that the y axis is in the strike direction. (c) The initial stress state is shown in map-view where the  $x'$  direction is the normal to the strike of the fault. (d) The resultant stress state is simply the superposition of the induced and the remote stress fields once the induced field has undergone the necessary rotation ( $\delta$ ). The angle  $\gamma$  then becomes the new orientation for the principal stress direction based on the stress tensor superposition.

## REFERENCES CITED

- Angelier, J., 1979, Determination of the mean principal directions of stresses for a give fault population, *Tectonophysics*, v. 56, p. T17–T26.
- Byerlee, J. D., 1979, Friction of rock: *Pure Applied Geophysics*, v. 116, p. 615–626.
- Castillo, D. A., and M. D. Zoback, 1994, Systematic variations in stress state in the southern San Joaquin Valley: inferences based on well-bore data and contemporary seismicity, *AAPG Bulletin*, v. 78, p. 1257–1275.
- Davis, T. L., and M. B. Lague, 1986, Seismic potential of the Pleito thrust system and the White Wolf fault, southern San Joaquin Valley, California: *EOS, Transactions, American Geophysical Union*, v. 67, p. 1223.
- Jaeger, J. C., and N. G. W. Cook, 1979, *Fundamentals of rock mechanics*, 3rd ed.: Chapman and Hall, New York, 593 p.
- Kanamori, H., and D. L. Anderson, 1975, Theoretical basis of some empirical relations in seismology: *Bulletin of the Seismological Society of America*, v. 65, p. 1073–1095.
- Malvern, L. E., 1969, *Introduction to the mechanics of a continuous medium*: Englewood Cliffs, New Jersey, Prentice-Hall, p. 226.
- Wallace, T. C., and K. Junkyoung, 1989, Inversion of complex seismic sources, *in* The effects of structure and source complexity on waveforms: crustal structure of Tibet and the recovery of complex seismic sources: *Geophysics Laboratory, Air Force Systems Command, Report GL-TR-89-0259*, 181 p.
- Webb, T. H., and H. Kanamori, 1985, Earthquake focal mechanisms in the eastern Transverse Ranges and the San Emigdio Mountains, southern California and evidence for a decollement: *Bulletin of the Seismological Society of America*, v. 75, p. 737–758.